Characterization and Application of Nanomaterials 2026, 9(3), 026190012.
https://doi.org/10.24294/can026190012

Article

Investigation of pinning effects and domain wall dynamics in magnetic micro- and nanopowders by spin-echo NMR using an additional magnetic video pulse

Grigor Mamniashvili*, Tatiana Gegechkori, Giorgi Donadze

Andronikashvili Institute of Physics, Ivane Javakhishvili Tbilisi State University, 6 Tamarashvili Street, 0177 Tbilisi, Georgia
* **Corresponding author:** Grigor Mamniashvili, mgrigor@rocketmail.com

CITATION

Mamniashvili G, Gegechkori T, Donadze G. Investigation of pinning effects and domain wall dynamics in magnetic micro- and nanopowders by spin-echo NMR using an additional magnetic video pulse. Characterization and Application of Nanomaterials. 2026; 9(3): 026190012. https://doi.org/10.24294/can026190012

ARTICLE INFO

Received: 09 May 2026
Accepted: 04 August 2026
Available online: 08 September 2026

Abstract: The behavior and pinning characteristics of domain walls in cobalt and lithium ferrite micropowders, as well as cobalt nanopowders, were investigated. The study employed the microscopic two-pulse spin-echo nuclear magnetic resonance technique with an additional magnetic video pulse applied between the radio-frequency (RF) pulses. This method yields two-pulse-echo suppression characteristics under magnetic video-pulse excitation, where the two-pulse-echo suppression signal is proportional to the domain wall velocity, similarly to observations from the magneto-optical Kerr effect (MOKE) and the Sixtus–Tonks technique. Unlike macroscopic approaches such as the magneto-optical Kerr effect and Sixtus–Tonks methods, this technique provides local, site-specific information about domain wall mobility and pinning strength. The obtained results may contribute to the development and optimization of magnetic micro- and nanopowder production technologies for applications including sensors, memory devices, rare-earth-free permanent magnets, water treatment systems, and other advanced technologies.

Keywords: cobalt; lithium ferrite; micropowders; nanopowders; NMR; two-pulse echo; magnetic video pulse

1. Introduction

The study of magnetism and magnetic materials is fundamental to the development of modern science and advanced technologies [1]. Nuclear magnetic resonance (NMR) in magnetically ordered systems was first described by Gossard and Portis in ferromagnetic cobalt [2]. Since that pioneering work, NMR has become one of the most powerful and informative techniques for studying magnetic materials [3,4].

NMR techniques are particularly effective for investigating the dynamics of domain walls (DWs) in magnetic micro- and nanostructures. Conventional magnetic characterization methods, such as the magneto-optical Kerr effect (MOKE) microscopy and magnetoresistance measurements, often provide only macroscopic or surface-sensitive information and may lack sufficient spatial or temporal resolution. In contrast, NMR enables microscopic and spatially localized probing of local magnetic structure and spin dynamics in such systems [4–9].

A key feature of NMR in magnetic materials is the presence of a strong hyperfine field at nuclear sites, which allows NMR signals to be observed even in the absence of an external magnetic field. In ferromagnets, the dominant contribution to the HF field arises from the effective hyperfine interaction produced by the polarization of s-electrons via the Fermi contact interaction associated with spontaneous magnetization [3]. The magnitude of the HF field typically reaches 10^5–10^6 Oe.

The observation of NMR in magnetic systems is further enhanced by the indirect action of the radio-frequency (RF) field on nuclear spins via its coupling to the electron magnetization. As a result, the effective resonant field acting on the nuclei is amplified by enhancement factors of approximately $\eta_d \sim 10^2$ inside domains and $\eta_w \sim 10^4$ inside domain walls. Consequently, the dominant contribution to the resonant absorption intensity arises from nuclei located within DWs, where the enhancement factor is particularly large. Under the NMR experimental conditions used (RF pulse power up to 1.5 W), the detected signal primarily originates from nuclei located in DWs. When an RF excitation pulse with amplitude H_1 is applied to a sample, the domain wall (DW) undergoes oscillations about its equilibrium position. In this case, even a small displacement of the DW is accompanied by a large rotation of the electronic magnetization M within the DW, resulting in a much greater RF pulse enhancement in the DWs than in the domains [3].

Because DWs can be displaced by applying an additional magnetic video pulse (MVP), NMR provides an effective tool for studying DW pinning and mobility [9]. The influence of MVPs on DW dynamics was first investigated in ferromagnetic metals such as Fe, Co, and Ni using NMR techniques [10]. It was demonstrated that applying an MVP between RF pulses causes a reduction in the spin-echo intensity proportional to the product of the MVP amplitude and duration. This attenuation results from inhomogeneous shifts of the NMR frequency at nuclear sites induced by DW displacement and reflects the anisotropy of the HF field within the wall.

Later, this method was extended to the investigation of MVP effects on nuclear spin-echo signals in a variety of ferro- and ferrimagnetic materials [11]. Earlier studies by Galt [12], employing the Sixtus method, also examined DW dynamics in single-crystal ferrites under MVP excitation.

These studies showed that the DW velocity, ν, depends linearly on the applied MVP field H:

$$\nu = S(H - H_0) \tag{1}$$

where S is the DW mobility and H_0 is the critical (pinning) field below which the DW remains stationary.

Even small DW displacements are accompanied by significant rotations of the magnetization vector M. The rotation angle of M within the DW is proportional to the wall displacement, leading to corresponding variations in the hyperfine field at nuclear sites due to the anisotropy of the hyperfine interaction inside the DW [4].

Similar linear relationships between DW velocity and applied magnetic field, as expressed in **Equation (1)**, have also been observed using the MOKE [13] and Sixtus–Tonks [14] techniques.

In recent years, considerable progress has been achieved in controlling magnetization switching in micro- and submicrometer magnetic structures, leading to new insights into magnetization reversal mechanisms. These investigations are highly important for applications in magnetoresistive random-access memory (MRAM) technologies, where DW displacement is considered one of the most promising mechanisms for localized magnetization switching.

The study of DW dynamics in confined geometries is of both fundamental and technological significance, particularly for emerging magnetic logic devices. This becomes especially important when the lateral dimensions of magnetic structures approach the intrinsic width of the DW [15].

Recently, interest in similar issues has been growing, e.g., [16–18].

In the present work, the dynamics of DWs and the pinning field in cobalt micro- and nanopowders are investigated using the microscopic NMR two-pulse spin-echo (TPE) technique [19]. In contrast to macroscopic approaches such as the MOKE [13] and the Sixtus–Tonks [14] methods, the NMR technique provides microscopic information about local DW behavior and pinning processes in magnetic micro- and nanostructures.

2. Experimental results and discussions

Measurements were carried out using a phase-incoherent spin-echo spectrometer operating in the frequency range of 40–400 MHz at 77 K and 300 K [19,20]. In the 40–220 MHz interval, a conventional self-excited oscillator was used, providing continuous frequency adjustment through variable inductors and tuning capacitors. For frequencies between 200 and 400 MHz, a serial Lecher-line generator with a two-wire transmission system was employed, incorporating two inductors with different turn numbers. For RF pulse durations ranging from 0.1 to 50 μs, the maximum RF magnetic field at the sample reached approximately 3.0 Oe, while the rise time remained below 0.15 μs. The receiver dead time was close to 1 μs.

A schematic representation of the experimental arrangement for simultaneous application of RF and MVP fields is presented in **Figure 1.**

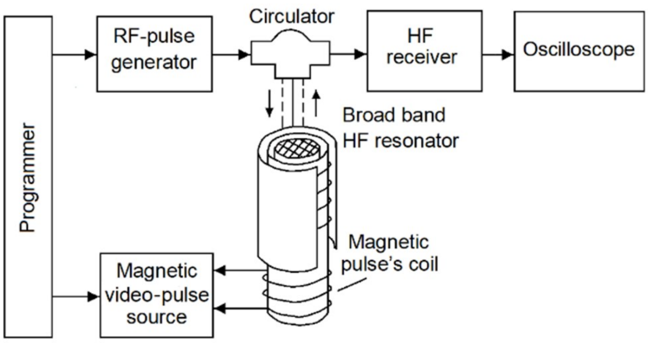

(**a**)

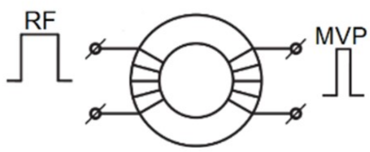

(**b**)

Figure 1. Scheme of the NMR experiment in the case of cobalt (**a**). NMR cell in the case of the lithium-zinc ferrite experiment (**b**).

The pulsed magnetic field was generated by a gated current stabilizer connected to an auxiliary copper coil with adjustable amplitude, allowing magnetic field pulses up to 500 Oe to be produced for samples approximately 10 mm in size.

The experiments were performed at temperatures of 77 and 300 K. Echo signal amplitudes were recorded both with and without the MVP field of amplitude H. The shape and position of the MVP were assessed using the 150 MHz frequency-band oscilloscope based on the current pulse through a 6-turn accessory copper coil. The MVP quality was sufficiently good to ensure a constant MVP threshold area over a wide range of pulse durations, from 0.5 to 5 μs.

Lithium–zinc ferrite samples with composition $Li_{0.5}Fe_{2.35}Zn_{0.15}O_4$ were prepared in ring-shaped form with diameters of 12–15 mm and a mass of 5.8 g. To enhance the echo signal intensity, the samples were enriched to 96.8% with the ^{57}Fe isotope. Polycrystalline cobalt powders produced by induction melting were also investigated, having an average grain size below 50 μm [20].

Additionally, cobalt nanopowders fabricated using electron-beam technology, with an average particle diameter of approximately 100 nm [21], were employed for sample preparation. Epoxy-encapsulated specimens were produced by placing the cobalt materials into polyethylene tubes filled with epoxy resin.

Figure 2 illustrates the action of the MVP between two RF pulses (a) and the ^{59}Co NMR spectrum recorded for cobalt micropowders at T = 77 K under optimal RF pulse power conditions with f_{nmr} = 217 MHz (b).

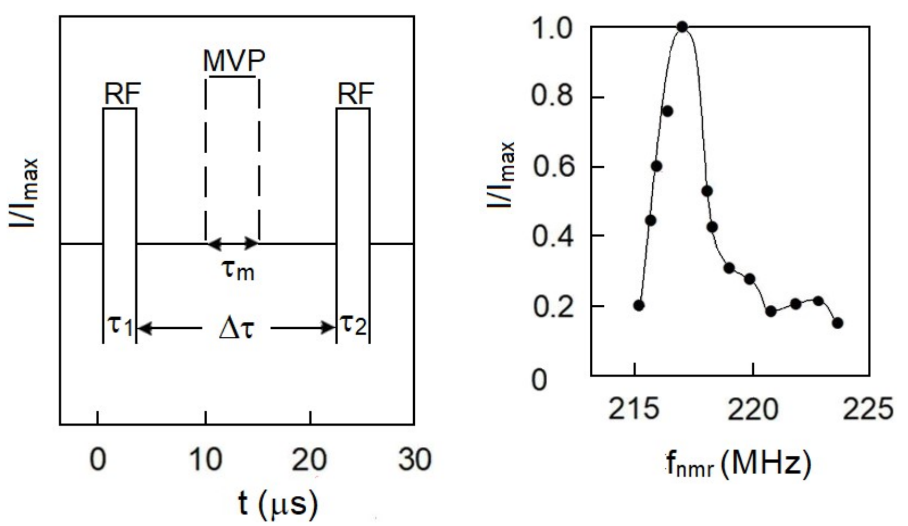

(**a**) (**b**)

Figure 2. MVP action between two RF pulses: τ_1 and τ_2 are the lengths of the first and second RF pulses, respectively; τ_{12} is the distance between these pulses and τ_m is the length of the magnetic video pulse (**a**), and the ^{59}Co NMR spectrum of cobalt micropowders recorded at T = 77 K under optimal RF pulse power conditions, f_{nmr} =217 MHz (**b**).

An oscillogram of the two-pulse spin-echo (TPE) signal obtained for cobalt micropowder samples is shown in **Figure 3.**

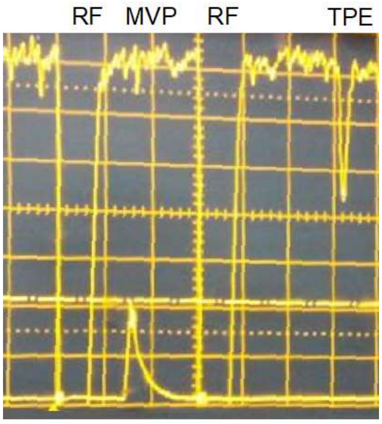

Figure 3. Oscillogram of the TPE signal in cobalt (upper trace). The lower trace corresponds to the wave-meter signal indicating the positions of the RF and MVP pulses, f_{nmr} = 217 MHz and T = 77 K. This oscillogram shows the dependence of the electrical signal in volts versus time (μs). The vertical size of each square corresponds to 2 volts, while the horizontal size corresponds to 10 μs.

Because the external RF field interacts with nuclei through electron spins, even a small displacement of the DW induces a substantial rotation of the electronic magnetization M. The rotation of M inside the DW is proportional to the magnitude of the wall displacement. This process is accompanied by changes in the local hyperfine field acting on nuclei within the DW due to magnetic anisotropy, and these changes are likewise proportional to the DW displacement.

The MVP amplitude at which echo intensity begins to decrease, corresponding to the onset of DW motion, can be associated with the DW pinning force. As shown in **Figure 4** (curves 1 and 2), the pinning force increases significantly when transitioning from cobalt micropowders to nanopowders. It is well known that reducing the cobalt grain size from approximately 1 μm to 150 nm substantially increases the coercive force due to size reduction and the growing influence of surface effects.

Figure 4 also shows the dependence of the degree of two-pulse echo suppression (TES), $\Delta I/I_{max}$, caused by DW displacement, on the MVP amplitude.

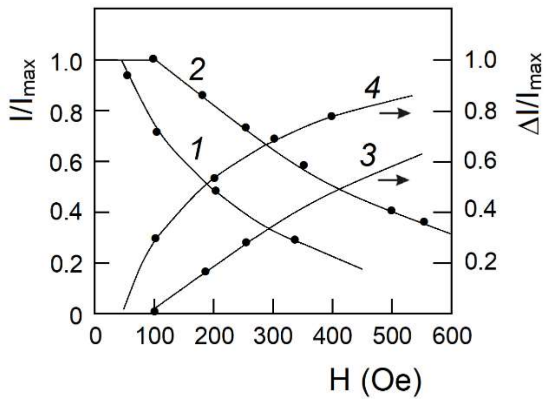

Figure 4. Dependence of the TPE signal produced by the combined action of MVP and two RF pulses (1 and 2) on the amplitude of the MVP with duration τ_m = 1 μs in cobalt micro- and nanopowders, respectively. The corresponding TES dependences

are shown by curves 3 and 4; f_{nmr} = 217 MHz and T = 77 K. NMR measurements were carried out with an accuracy of approximately 1%.

It is of interest to determine the form of the corresponding MVP-effect diagrams in lithium ferrite, due to its significantly lower magnetic anisotropy and higher DW mobility.

As reported in [22], the NMR spectrum of a lithium ferrite single crystal consists of two well-resolved lines: the low-frequency line is associated with tetrahedral A sites, while the high-frequency line corresponds to octahedral B sites. At T = 300 K, the fine structure of the spectrum is not resolved, whereas at 77 K and 4.2 K, four and five lines are observed, respectively.

Figure 5 presents the NMR spectrum of lithium ferrite (a) together with the amplitude dependences of the TPE and TES signals for both local maxima of the spectrum (b). A comparison of the TES dependences in cobalt and lithium ferrite with the DW velocity dependences on MVP amplitude obtained via the Sixtus method [12] (**Figure 6**) reveals a clear qualitative correspondence between these quantities. Similar behavior was later reported using MOKE [13] and Sixtus–Tonks [14] techniques for planar permalloy nanowires and amorphous $Fe_{77.5}Si_{7.5}B_{15}$ microwires, respectively

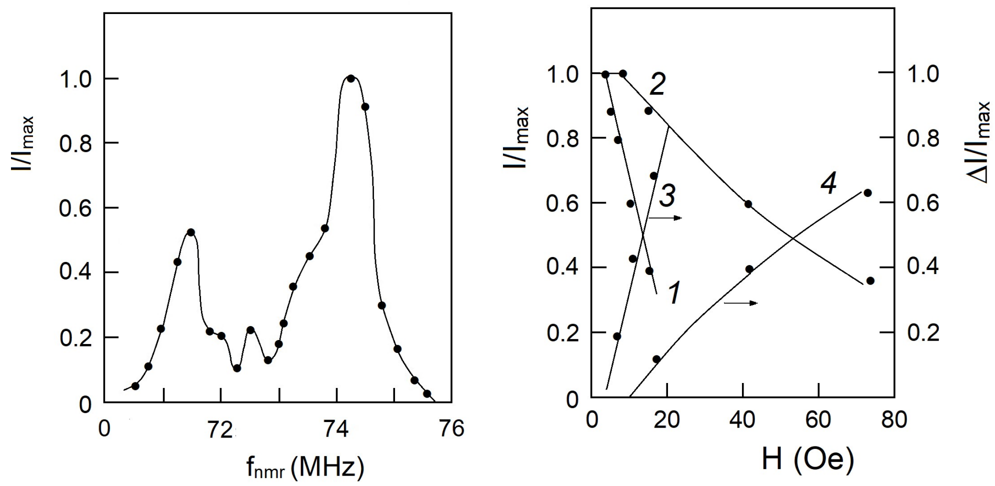

(**a**) (**b**)

Figure 5. ^{57}Fe NMR spectrum of lithium–zinc ferrite (**a**). Amplitude dependences of the TPE and TES signals as functions of MVP excitation are shown in panel (**b**). Curves 1 and 2 correspond to the B and A sites with resonance frequencies of 74 MHz and 71 MHz for the TPE signal, respectively, while curves 3 and 4 show the corresponding TES dependences. The MVP duration is τ_m = 0.5 μs, and the temperature is T = 77 K.

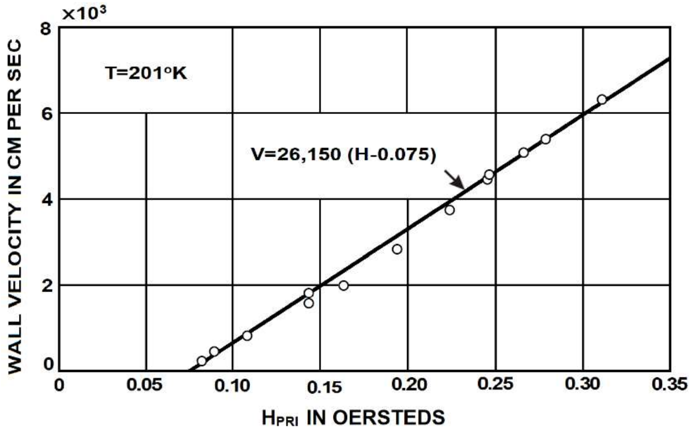

Figure 6. Domain wall velocity in a single-crystal ferrite under MVP excitation measured using the Sixtus method [12].

The main features of the experimentally observed results can be understood qualitatively as follows. It is well established that when an RF excitation pulse with amplitude H_1 is applied, the DW performs the oscillations about its equilibrium position (0–0), as illustrated in **Figure 7** [4]. In this regime, the NMR signal originates from nuclei located in the central region of the DW, having an effective length L. Accordingly, the NMR signal intensity is proportional to the number of nuclei within this region and therefore to L.

When an MVP pulse H is applied, the DW is displaced by an amount Δx and then oscillates during the pulse duration τ_m around a new equilibrium position (o′–o′). This displacement excludes a portion of nuclei from contributing to the resonance process, leading to a decrease in the NMR signal proportional to Δx. Since the displacement is proportional to the DW velocity ν, this provides a natural explanation for the observed similarity between the TES dependences and the DW velocity dependence ν(H) (**Figure 6**).

Thus, the variation of the TES signal can be expressed as:

$$\Delta I/I \sim \Delta x = \upsilon\, \tau_m = S(H - H_0)\tau_m \quad (2)$$

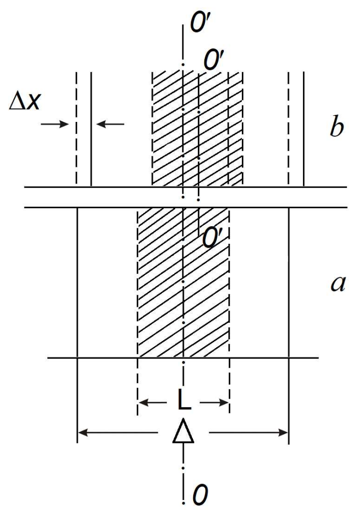

Figure 7. Schematic illustration of a DW with width Δ: (**a**) equilibrium configuration, and (**b**) displacement by Δx induced by an MVP field amplitude H.

Next, we examine how the DW pinning field H_0 depends on the MVP amplitude H. **Figure 8** shows the corresponding dependence of the TPE intensity on MVP amplitude for two fixed pulse durations τ_m in cobalt micropowders.

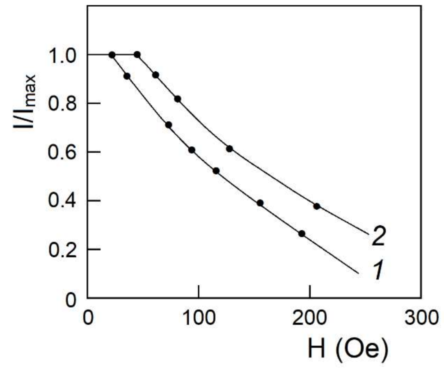

Figure 8. Dependence of the TPE signal intensity under MVP excitation for τ_m = 3 μs (1) and τ_m = 1.5 μs (2), measured at an NMR frequency of f_{nmr} = 217 MHz.

Figure 9 presents similar dependences of the TPE intensity on τ_m for three fixed MVP amplitudes in cobalt micropowders.

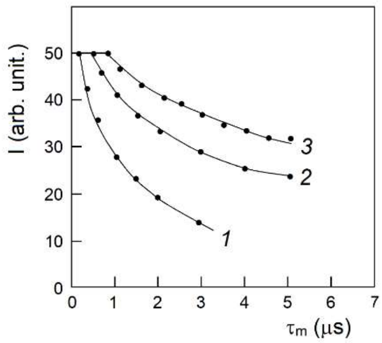

Figure 9. Dependence of the TPE intensity on τ_m for three constant MVP amplitudes (1–3: 200, 100, and 50 Oe, respectively), f_{nmr} = 213 MHz, T = 300 K.

Figure 10 summarizes the resulting dependence of the DW pinning field H_0, defined at the onset of TPE suppression under MVP excitation, as a function of pulse duration.

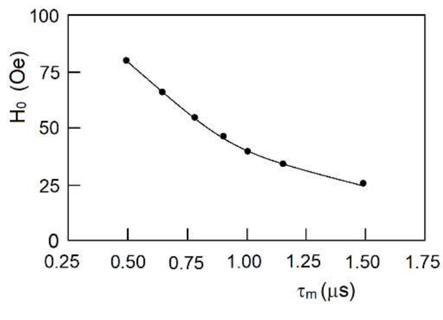

Figure 10. Dependence of the DW pinning field H_0 on the MVP pulse duration τ_m for cobalt micropowders, f_{nmr} = 217 MHz, T = 77 K.

The results indicate that the pinning field follows the relation H_0 τ_m = const. In other words, the threshold condition for TPE suppression corresponds to a constant MVP "area" (field–time product).

This behavior can be interpreted within the framework of the one-dimensional DW model [23], where the displacement Δx of DWs under a short MVP pulse of amplitude H and duration τ_m is described by:

$$x = C \cdot H \cdot \tau_m, \quad (3)$$

where C is a material-dependent constant. Accordingly, each threshold condition corresponds to the same DW displacement, which can be associated with the characteristic width of the potential well responsible for DW pinning.

A similar relationship between H_0 and τ_m was previously reported using the magneto-optical Kerr effect in permalloy films [24].

It should be noted that for τ_m = 1 μs, the DW pinning field H_0 is comparable in magnitude to the coercive field H_c. However, this correspondence is not universal, since H_0 depends on pulse duration. This is because H_0 is determined by the constant threshold condition H_0 τ_m = const, making it inversely proportional to τ_m.

Estimates of DW velocities and pinning fields in cobalt micro- and nanopowders, together with advances in their synthesis, suggest their potential for applications in rare-earth-free permanent magnets, memory devices, sensors, and related technologies. In particular, these results and the described methodology may also be relevant for improving the photocatalytic and magnetic properties of TiO_2 micro- and nanopowders decorated with Ni and Co nanoclusters [25] employed in water purification technologies.

The obtained results refer to promising areas of scientific research with great potential for practical application [26–28].

3. Conclusion

The dynamics and pinning of domain walls in cobalt micropowders, lithium ferrite, and cobalt nanopowders were investigated using a microscopic NMR two-pulse spin-echo technique with an additional magnetic video pulse applied between the RF pulses. This method yields two-pulse echo suppression characteristics under magnetic video pulse excitation, where the two-pulse-echo suppression signal is proportional to domain wall velocity, similar to observations from magneto-optical Kerr effect and Sixtus–Tonks techniques.

Unlike macroscopic approaches such as magneto-optical Kerr effect and Sixtus–Tonks methods, this technique provides local, site-specific information on domain wall mobility and pinning strength. Such insights may be useful for optimizing the fabrication of micro- and nanopowders of magnetic materials for applications in sensors, memory devices, rare-earth-free permanent magnets, and related technologies.

Author contributions: GM: conceptualization, methodology; TG: methodology, investigation, writing; GD: investigation.

Funding: This work was supported by Shota Rustaveli National Science Foundation of Georgia (SRNSFG) [AR-25-1485, Compact synergetic water purification module].

Availability of data: The raw data supporting the conclusions of this article will be made available by the authors upon reasonable request, without undue reservation.

Conflict of interest: The authors declare no conflict of interest.

References

1. Coey JM. Magnetism and magnetic materials. Cambridge University Press; 2010.
2. Gossard AC, Portis AM. Observation of nuclear resonance in a ferromagnet. Physical Review Letters. 1954; 3(4), 164-166. doi: 10.1103/PhysRevLett.3.164
3. Turov EA, Petrov MP. Nuclear magnetic resonance in ferro- and antiferromagnetics. Hoboken, New Jersey: John Wiley & Sons, Inc.; 1972:206.
4. Guimarães AP. Magnetism and magnetic resonance in solids. New York: Wiley; 1998.
5. Meny C, Panissod P. Nuclear magnetic resonance in ferromagnets: Ferromagnetic nuclear resonance; a very broadband approach. Annual Reports on NMR Spectroscopy. 2021; 103, 47-96. doi: 10.1016/bs.arnmr.2021.02.001
6. Scholzen P, Lang G, Andreev AS, et al. Magnetic structure and internal field nuclear magnetic resonance of cobalt nanowires. Physical Chemistry Chemical Physics. 2022; 24(19), 11898-11909. doi: 10.1039/D1CP05164D
7. Mamniashvili GI, Gegechkori TO, Zedginidze TI, et al. Chemical synthesis of cobalt nanowires in an external magnetic field and their characterization by NMR. Journal of Applied Spectroscopy. 2024; 91(1), 21-24. doi: 10.1007/s10812-024-01685-0
8. Shmyreva AA, Kirillov VE, Dzhangurazov EB, et al. Inhomogeneous magnetic structure of the metallic FM part of Co/CoO nanoparticles by the ^{59}Co nuclear magnetic resonance method. Russian Journal of Physical Chemistry B. 2023; 17(3), 764-773. doi: 10.1134/S1990793123030120
9. Gavasheli T, Mamniashvili G, Gegechkori T, et al. Magnetic video-pulse impact on NMR spin echo signals of nuclei located in domain walls of magnets. IEEE XXVIII International Seminar/Workshop on Direct and Inverse Problems of Electromagnetic and Acoustic Wave Theory (DIPED). 2023; 1, 176-179. doi: 10.1109/DIPED59408.2023.10269510
10. Weger M, Hahn EL, Portis AM. Transient excitation of nuclei in ferromagnetic metals. Journal of Applied Physics. 1961; 32(3), S124-S125. doi: 10.1063/1.2000373
11. Rassvetalov LA, Levitski AB. Influence of a pulsed magnetic field on the nuclear spin echo in some ferromagnets and ferrimagnets. Soviet Physics Solid State Physics. 1981; 23(11), 3354-3359.
12. Galt JK. Motion of individual domain walls in a nickel-iron ferrite. Bell System Technical Journal. 1954; 33(5), 1023-1054. doi: 10.1002/j.1538-7305.1954.tb02363.x
13. Atkinson D, Allwood DA, Faulkner CC, et al. Magnetic domain wall dynamics in a permalloy nanowire. IEEE Transactions on Magnetics. 2003; 39(5), 2663-2665. doi: 10.1109/TMAG.2003.815548
14. Varga R, Richter K, Zhukov A, et al. Domain wall propagation in thin magnetic wires. IEEE Transactions on Magnetics. 2008; 44(11), 3925-3930. doi: 10.1109/TMAG.2008.2001997
15. Csaba G. Spin-based computing devices. Cham: Springer Switzerland AG; 2025.
16. Gavasheli TA, Mamniashvili GI. Study of domain wall pinning in magnetized cobalt composite based on epoxy matrix by NMR and RF magnetometry. Technical Physics Letters. 2025; 51(1), 66-68. doi: 10.61011/TPL.2025.01.60142.20050
17. Yang L. Pinning effect on current-induced domain wall motion in nanostrip. East Asian Journal on Applied Mathematics. 2017; 7(4), 837-851. doi: 10.4208/eajam.181016.300517d
18. Yan R, Lin Q, You K, et al. Construction strategies and recent advances of flexible EMI phase change composites. Soft Science. 2025; 5(1), N-A. doi: 10.205017/ss.2024.66
19. Gavasheli AM, Mamniashvili GI, Shermadini ZG, et al. Investigation of the pinning and mobility of domain walls in cobalt micro- and nanowires by the nuclear spin echo method under the additional influence of a magnetic video-pulse. Journal of Magnetism and Magnetic Materials. 2020; 500, 166310. doi: 10.1016/j.jmmm.2019.166310
20. Kiliptari IG, Tsifrinovich VI. Single-pulse nuclear spin echo in magnets. Physical Review B. 1998; 57, 11554-11564. doi: 10.1103/PhysRevB.57.11554
21. Mamniashvili G, Gegechkori T, Okrosashvili M, et al. Production of cobalt nanopowders by electron-beam technology and their NMR and magnetometry study. Journal of Magnetism and Magnetic Materials. 2015; 373, 177-182. doi: 10.1016/j.jmmm.2014.03.058

22. Doroshev VD, Klochan VA, Kovtun NM, et al. The effect of dipole and anisotropic hyperfine fields on NMR of Fe^{57} in lithium ferrite $Li_{0.5}Fe_{2.5}O_4$. Physica Status Solidi A. 1972; 9(2), 679-689. doi: 10.1002/pssa.2210090234
23. Konishi S, Mizuno K, Watanabe F, et al. Domain wall displacement under pulsed magnetic field. AIP Conference Proceedings. 1976; 34(1), 145-147. doi: 10.1063/1.2946043
24. Bartran D, Bourne H. Domain wall velocity and interrupted pulse experiments. IEEE Transactions on Magnetics. 1973; 9(4), 609-613. doi: 10.1109/TMAG.1973.1067703
25. Gegechkori T, Mamniashvili G, Gagnidze T, et al. Photocatalytic and magnetic properties of TiO_2 micro- and nano-powders decorated by magnetic cocatalysts. Engineering, Technology and Applied Science Research. 2023; 13(5), 11924-11931. doi: 10.48084/etasr.6244
26. Lee T, Jeong S, Kim KJ, et al. Position-reconfigurable pinning for magnetic domain wall motion. Scientific Reports. 2023; 13(1), 6791. doi: 10.1038/s41598-023-34040-y
27. Rahaman H, Kumar D, Chung HJ, et al. Diode characteristics in magnetic domain wall devices via geometrical pinning for neuromorphic computing. ACS Applied Materials & Interfaces. 2023; 15(12), 15832-15838. doi: 10.1021/acsami.2c20905
28. Durner CA, Migliorini A, Jeon JC, et al. Reconfigurable magnetic inhibitor for domain wall logic and neuronal devices. ACS Nano. 2025; 19(5), 5316-5325. doi: 10.1021/acsnano.4c12503